International Journal of Mathematical Archive-2(12), 2011, Page: 2625-2639
Available online through www.ijma.info ISSN 2229 – 5046

RUN-UP FLOW OF A RIVILIN-ERICKSEN FLUID THROUGH A POROUS MEDIUM IN A CHANNEL

Dr. V. Sugunamma[1*], M. Sneha Latha[2] and N. Sandeep[3]

[1]Associate Professor, Department of mathematics, S. V. University, Tirupati, A.P., India
[2,3]Research Scholars, Department of mathematics, S. V. University, Tirupati, A.P., India
E-mail: vsugunar@yahoo.co.in

(Received on: 19-11-11; Accepted on: 10-12-11)

ABSTRACT

In this paper we analyze the start-up flow of an incompressible Viscoelastic Rivlin-Ericksen fluid. The initial flow is assumed due to the movement of boundaries. At an instant of time t, the boundaries are suddenly brought to rest and the flow is maintained due to a prescribed pressure gradient. The governing equations are solved applying Laplace Transform Technique and the flow characteristics are discussed for different flow variables. The analysis is carried out by considering the pressure gradient in the form c(1 + f(t)) where f(t) is taken in the following forms a) γt b) $e^{-\gamma t}$ c) $te^{-\gamma t}$ d) 0 which corresponds to constant pressure gradient.

Key Words: *Rivlin-Ericksen fluid, Viscoelastic, Porous Medium.*

INTRODUCTION:

Flows through porous medium are of principal interest in the fields of agricultural engineering, underground water resources and seepage of water in river beds, filtration and purification processes in chemical engineering, petroleum technology to study the movement of natural gas, oil and water through the oil reservoirs. A porous medium is a solid which contains a number of small holes distributed throughout the solid. These holes may be effective or ineffective. Fluid can pass through effective holes and these holes contribute towards the porosity of the material. Fluid cannot pass through ineffective holes. Some of the examples of porous medium are a pack of sand, cotton and woolen packing, wood dust, soil, leather, sandstone and foamed plastics. The porosity of the material is defined as the fraction of the total volume of the material which is actually occupied by the holes. In the year 1856 Darcy [4] gave an empirical formula from his experimental results on flows of water through porous medium

$$\mathbf{v} = -k/\mu \quad (\nabla P - \rho\mathbf{F}) \tag{I}$$

where k is the permeability of the material, ρ is the density, **v** is the velocity vector and **F** is the force, μ is the coefficient of viscosity.

The equation (I) can also be written as

$$\nabla < p > = \rho\, g - \frac{\mu}{k} u \tag{II}$$

This equation is of the potential flow form and is valid when *k* is very large. However, in many practical problems the permeability is small near the boundary i.e., the particles are loosely packed so that there .exists a boundary layer thickness very near to the surface. The existence of this boundary layer thickness is experimentally demonstrated by Beavers and Joseph [2]. Taking into consideration the above aspect, the equation (II) can be written in the form

$$\nabla < p > = \rho\, g - \frac{\mu}{k} u + \mu \nabla^2 u \tag{III}$$

This boundary layer type equation for flow through porous media was postulated by Brinkman [3]

The study of run-up flows is gaining importance due to its wide applications in different technologies. Such phenomenon arises in petrochemical engineering, lubrication technology, irrigation systems, water supply and bio-fluid mechanics where the pressure gradient is suddenly withdrawn from the steady state flow which henceforth gains unsteadiness due to extraneous influence. Researchers in this field are initiated for the first time by Kazakia and Rivlin [5] in which they investigated run-up flow in an incompressible isotropic Viscoelastic fluid contained between two infinite rigid parallel plates. Rivlin [9] also discussed run-up and spin-up flow in a Viscoelastic fluid between two

Corresponding author: Dr. V. Sugunamma[1], *E-mail: vsugunar@yahoo.co.in

infinite parallel plates containing Maxwell fluid initially at rest. They have studied the fluid motion resulting from sudden velocities given to the plates and subsequently held constant. Pattabhi Ramacharyulu and Appala Raju [7] have studied run-up flow in a generalized porous medium. Ramakrishna [8] discussed a similar problem related to the flow of a dusty viscous fluid in a conduit choosing parallel plate geometry and cylindrical geometry. Raji Reddy and Sambasiva Rao [101 analyzed run-up flow of viscous incompressible fluid through a rectangular pipe, a pipe of equilateral triangular cross-section, parallel plate channel and a circular cylinder. They solved the problem using ADI numerical technique. Basha [6] extended the analysis of Raji Reddy and Sambasiva Rao [10] by considering Viscoelastic Rivlin-Erickson fluid between parallel plates. He extended this study by taking a second order Rivlin-Ericksen Viscoelastic fluid between parallel porous plates subjected to a constant suction. Anderson *et al* [1] studied run-up flow of a viscous fluid in a porous medium channel. The run-up flow is discussed in two cases by maintaining a constant pressure gradient and a constant flow rate. The time histories of the centerline velocity and the wall friction are calculated together with time varying velocity profiles.

In this paper we have studied the start-up flow of an incompressible Viscoelastic Rivlin-Ericksen fluid. The initial flow is assumed due to the movement of boundaries. At an instant of time t, the boundaries are suddenly brought to rest and the flow is maintained due to a prescribed pressure gradient. The governing equations are solved applying Laplace Transform Technique and the flow characteristics are discussed for different flow variables. The analysis is carried out by considering the pressure gradient in the form $c(1 + f(t))$ where $f(t)$ is taken in the following forms a) γt b) $e^{-\gamma t}$ c) $te^{-\gamma t}$ d) 0 which corresponds to constant pressure gradient.

FORMULATION OF THE PROBLEM:

We consider the time-dependent and unidirectional flow of an incompressible Viscoelastic Rivlin-Ericksen fluid through a porous medium in an infinitely long channel bounded by two parallel plane boundaries. The solid matrix is treated as homogeneous with respect to porosity characteristics.

The governing equation of the flow in the Cartesian coordinates (x′, y′, z′) are $\dfrac{\partial w'}{\partial z'} = 0$ (1)

$$\rho \frac{\partial w'}{\partial t'} = -\frac{\partial p'}{\partial z'} + \mu \frac{\partial^2 w'}{\partial y'^2} + \alpha_1 \frac{\partial^3 w'}{\partial t' \partial y'^2} - \frac{\mu}{k} w' \quad (2)$$

Where (0, 0, w′) is the velocity, ρ is the density of the fluid, μ is the coefficient of viscosity, p′ is the pressure, *k* is the permeability parameter, t′ is the time and α_1 is the coefficient of kinematic Viscoelacity.

We introduce the non-dimensional variable

$$(y', z') = h\,(y,z)\,,\ t' = \left(\frac{h}{u}\right) t$$
$$w' = uw,\ p' = \rho u^2 p \quad (3)$$

Where *u* is a characteristic velocity, *h* is half width of the channel.

The governing equations in the non-dimensional form reduce to

$$\frac{\partial w}{\partial t} = -\frac{\partial p}{\partial z} + \frac{1}{R}\,\frac{\partial^2 w}{R\,\partial y^2} + \alpha_0\,\frac{\partial^3 w}{\partial t \partial y^2} - \frac{D^{-1}}{R}\,w \quad (4)$$

Where

$R = \dfrac{\rho u h}{\mu}$ (Reynolds number)

$D^{-1} = \dfrac{h^2}{k}$ (Darcy parameter)

$\alpha_0 = \dfrac{\alpha_1}{\rho h^2}$ (Viscoelastic parameter)

We assume that initially the flow is steady due to the movement of the upper plate in the absence of an external pressure gradient. The steady state momentum equation obtained from (4) is

$$\frac{\partial^2 w}{\partial y^2} - D^{-1} w = 0 \quad (5)$$

The corresponding boundary conditions in non-dimensional form are

w = 0 at y = -1 and
w = 1 at y = +1 (6)

On solving equation (5) and using the boundary conditions (6) we obtain the velocity

$$w = \frac{\sinh a\,(1+y)}{\sinh a}$$

Where $a^2 = D^{-1}$ (7)

Now the boundaries are brought to rest and the flow is maintained by prescribing a pressure gradient

$$-\frac{\partial p}{\partial z} = c(1+f(t)) \tag{8}$$

Where *c* is constant.

The initial condition is

$$w = \frac{\sinh a\,(1+y)}{\sinh a} \quad at \quad t=0$$

The boundary conditions are given by

w = 0 at y = +1
w = 0 at y = -1 (9)

(9) Represents the no-slip condition.

Solution of the Problem:

We solve the governing equation (4) using the Laplace Transform technique.

Let $\overline{w}\,(y,s),\ \bar{f}\,(y,s)$ be the Laplace Transform with respect to't' of w(y, t), f (t) respectively given by the definition.

$$\left[\overline{w}\,(y,s),\ \bar{f}\,(y,s)\right] = \int_0^\infty e^{-st}\left[w(y,t), f\,(t)\right]dt \tag{10}$$

Where s is the transform parameter.

Taking Laplace Transform on both sides, equation (4) transforms to

$$\frac{d^2\,\overline{w}}{dy^2} - \frac{Rs+a^2}{1+\alpha_0\,Rs}\overline{w} = \frac{R}{1+\alpha_0\,Rs}\left[(\alpha_0\,a^2-1)\,\frac{\sinh a\,(1+y)}{\sinh 2\,a} - c\left(\frac{1}{s}+\bar{f}\,(s)\right)\right] \tag{11}$$

The transformed boundary conditions are

$\overline{w}$ = 0 at y = +1
$\overline{w}$ = 0 at y = -1 (12)

Solving (11) using the boundary conditions (12) we get

$$\overline{w} = \frac{1}{s}\left[\frac{\sinh a(1+y)}{\sinh 2a} - \frac{\sinh\ \beta(1+y)}{\sinh 2\beta}\right] + \frac{cR}{Rs+D^{-1}}\left(\frac{1}{s}+\bar{f}\,(s)\right)\left[\frac{\cosh\ \beta y}{\cosh\ \beta} - 1\right] \tag{13}$$

Where $\beta = \dfrac{\sqrt{Rs+a^2}}{\sqrt{1+\alpha_0\,Rs}}$

Taking the inverse Laplace transform of (13), the expression for velocity can be obtained.

The shear stress (τ) at the walls is calculated using the formula

$$\tau = \left(\frac{\partial w}{\partial y}\right) \tag{14}$$

The flow rate is calculated using the formula

$$Q = \int_{-1}^{+1} w\,dy \tag{15}$$

We obtain the solution of the problem by considering the different forms of pressure gradient in the following cases.

Case: I

When the pressure gradient is $-\dfrac{\partial p}{\partial z} = c(1+\gamma t)$, where γ is a constant i.e., the pressure gradient is a linear function of time.

The equation (3.2) takes the form

$$\overline{w} = \frac{1}{s}\left[\frac{\sinh a(1+y)}{\sinh 2a} - \frac{\sinh \beta(1+y)}{\sinh 2\beta}\right] + \frac{cR}{Rs + D^{-1}}\left(\frac{1}{s}+\frac{\gamma}{s^2}\right)\left[\frac{\cosh \beta y}{\cosh \beta} - 1\right] \tag{16}$$

Taking Inverse Laplace Transform of the above equation we get w(y, t) as

$$w(y,t) = \frac{cR}{D^{-1}}(1+\gamma)\left[\frac{\cosh ay}{\cosh a} - 1\right] + \sum_{n=0}^{\infty}\frac{(-1)^n e^{S_n t}\, n\pi(1+\alpha_0 Rs_n)^2}{2Rs_n(1-\alpha_0 a^2)} \sin\frac{n\pi}{2}(1+y)$$

$$+ c\left(1+\frac{\gamma}{s_n'}\right)\sum_{n=0}^{\infty}\frac{(-1)^n e^{S_n' t}(2n+1)\pi(1+\alpha_0 Rs_n')^2}{S_n'(R-\alpha_0 D^{-1}a^2)(Rs_n' + D^{-1})}\cos(2n+1)\frac{\pi}{2}y \tag{17}$$

Where $S_n = \dfrac{-\left[4a^2 + (2n+1)^2\pi^2\right]}{R\left[4+(2n+1)^2\pi^2\alpha_0\right]}$ *and* $S_n' = \dfrac{-\left[4a^2 + n^2\pi^2\right]}{R\left[4+n^2\pi^2\alpha_0\right]}$

The Shear stress τ on the upper wall is

$$(\tau)_{y=+1} = \frac{cR}{D^{-1}}(1+\gamma)\left[\frac{a\sinh a}{\cosh a}\right] + \sum_{n=0}^{\infty}\frac{e^{S_n t}\, n\pi(1+\alpha_0 Rs_n)^2}{4Rs_n(1-\alpha_0 a^2)}$$

$$-c\left(1+\frac{\gamma}{S_n'}\right)\sum_{n=0}^{\infty}\frac{(-1)^n e^{S_n' t}(2n+1)\pi(1+\alpha_0 Rs_n')^2}{2S_n'(R-\alpha_0 D^{-1}a^2)(Rs_n' + D^{-1})}\sin(2n+1)\frac{\pi}{2} \tag{18}$$

The Shear stress τ on the lower wall is

$$(\tau)_{y=-1} = \frac{cR}{D^{-1}}(1+\gamma)\left[\frac{a\sinh a}{\cosh a}\right] + \sum_{n=0}^{\infty}\frac{e^{S_n t}\, n\pi(1+\alpha_0 Rs_n)^2}{4Rs_n(1-\alpha_0 a^2)}$$

$$+c\left(1+\frac{\gamma}{S_n'}\right)\sum_{n=0}^{\infty}\frac{(-1)^n e^{S_n' t}(2n+1)\pi(1+\alpha_0 Rs_n')^2}{2S_n'(R-\alpha_0 D^{-1}a^2)(Rs_n' + D^{-1})}\sin(2n+1)\frac{\pi}{2} \tag{19}$$

The flow rate Q is given by

$$Q = \frac{2cR(1+\gamma)}{D^{-1}}\left[\frac{\sinh a}{a\cosh a} - 1\right] + \sum_{n=0}^{\infty}\frac{e^{S_n t}\, n\pi(1+\alpha_0 Rs_n)^2}{Rs_n(1-\alpha_0 a^2)}[1-(-1)^n]$$

$$+c\left(1+\frac{\gamma}{S_n'}\right)\sum_{n=0}^{\infty}\frac{(-1)^n\, 4e^{S_n t}\,(1+\alpha_0 Rs_n')^2}{S_n'\,(R-\alpha_0 D^{-1} S_n')\,(Rs_n'+D^{-1})}\sin(2n+1)\frac{\pi}{2} \tag{20}$$

The centerline velocity at y = 0 is given by

$$w(y=0)=\frac{cR(1+\gamma)}{D^{-1}}\left[\frac{1}{\cosh a}-1\right]+\sum_{n=0}^{\infty}\frac{(-1)^n e^{S_n t}\, n\pi(1+\alpha_0 Rs_n)^2}{Rs_n(1-\alpha_0 a^2)}\sin\frac{n\pi}{2}$$

$$+c\left(1+\frac{\gamma}{S_n'}\right)\sum_{n=0}^{\infty}\frac{(-1)^n e^{S_n t}\,(1+\alpha_0 Rs_n')^2}{S_n'\,(R-\alpha_0 D^{-1} S_n')\,(Rs_n'+D^{-1})} \tag{21}$$

Case: II

When the pressure gradient is $-\dfrac{\partial p}{\partial z}=c\,(1+e^{-\gamma t})$.

The equation (3.2) takes the form

$$\overline{w}=\frac{1}{s}\left[\frac{\sinh a(1+y)}{\sinh 2a}-\frac{\sinh \beta(1+y)}{\sinh 2\beta}\right]+\frac{cR}{Rs+D^{-1}}\left(\frac{1}{s}+\frac{1}{s+\gamma}\right)\left[\frac{\cosh \beta y}{\cosh \beta}-1\right] \tag{22}$$

Taking Inverse Laplace Transform we get w (y,t) as

$$w(y,t)=\frac{cR}{D^{-1}}(1+\gamma)\left[\frac{\cosh ay}{\cosh a}-1\right]+\sum_{n=0}^{\infty}\frac{(-1)^n e^{S_n t}\, n\pi(1+\alpha_0 Rs_n)^2}{2Rs_n(1-\alpha_0 a^2)}\sin\frac{n\pi}{2}(1+y)$$

$$+\,c\left(\frac{1}{s_n'}+\frac{1}{s_n'+\gamma}\right)\sum_{n=0}^{\infty}\frac{(-1)^n e^{S_n t}\,(2n+1)\pi(1+\alpha_0 Rs_n')^2}{(R-\alpha_0 D^{-1}a^2)\,(Rs_n'+D^{-1})}\cos(2n+1)\frac{\pi}{2}y \tag{23}$$

The Shear stress τ on the upper wall is

$$(\tau)_{y=+1}=\frac{cR}{D^{-1}}(1+\gamma)\left[\frac{a\sinh a}{\cosh a}\right]+\sum_{n=0}^{\infty}\frac{e^{S_n t}\, n\pi(1+\alpha_0 Rs_n)^2}{4Rs_n(1-\alpha_0 a^2)}$$

$$-c\left(\frac{1}{s_n'}+\frac{1}{s_n'+\gamma}\right)\sum_{n=0}^{\infty}\frac{(-1)^n e^{S_n t}\,(2n+1)\pi(1+\alpha_0 Rs_n')^2}{2(R-\alpha_0 D^{-1}a^2)\,(Rs_n'+D^{-1})}\sin(2n+1)\frac{\pi}{2} \tag{24}$$

The Shear stress τ on the lower wall is

$$(\tau)_{y=-1}=\frac{cR}{D^{-1}}(1+\gamma)\left[\frac{a\sinh a}{\cosh a}\right]+\sum_{n=0}^{\infty}\frac{e^{S_n t}\, n\pi(1+\alpha_0 Rs_n)^2}{4Rs_n(1-\alpha_0 a^2)}$$

$$+c\left(\frac{1}{s_n'}+\frac{1}{s_n'+\gamma}\right)\sum_{n=0}^{\infty}\frac{(-1)^n e^{S_n t}\,(2n+1)\pi(1+\alpha_0 Rs_n')^2}{2(R-\alpha_0 D^{-1}a^2)\,(Rs_n'+D^{-1})}\sin(2n+1)\frac{\pi}{2} \tag{25}$$

The flow rate Q is given by

$$Q = \frac{2cR(1+\gamma)}{D^{-1}}\left[\frac{\sinh a}{a\cosh a}-1\right]+\sum_{n=0}^{\infty}\frac{e^{S'_n t}\, n\pi(1+\alpha_0 Rs_n)^2}{Rs_n(1-\alpha_0 a^2)}[1-(-1)^n]$$

$$+c\left(\frac{1}{s_n'}+\frac{1}{s_n'+\gamma}\right)\sum_{n=0}^{\infty}\frac{(-1)^n 4e^{S_n t}(1+\alpha_0 Rs_n')^2}{S_n'(R-\alpha_0 D^{-1}S_n')(Rs_n'+D^{-1})}\sin(2n+1)\frac{\pi}{2} \tag{26}$$

The centerline velocity at y = 0 is given by

$$w(y=0)=\frac{cR(1+\gamma)}{D^{-1}}\left[\frac{1}{\cosh a}-1\right]+\sum_{n=0}^{\infty}\frac{(-1)^n e^{S_n t}\, n\pi(1+\alpha_0 Rs_n)^2}{Rs_n(1-\alpha_0 a^2)}\sin\frac{n\pi}{2}$$

$$+c\left(\frac{1}{s_n'}+\frac{1}{s_n'+\gamma}\right)\sum_{n=0}^{\infty}\frac{(-1)^n e^{S'_n t}(2n+1)\pi(1+\alpha_0 Rs_n')^2}{(R-\alpha_0 D^{-1}S_n')(Rs_n'+D^{-1})} \tag{27}$$

Case: III

When the pressure gradient is $-\frac{\partial p}{\partial z}=c(1+te^{-\gamma t})$.

The equation (3.2) takes the form

$$\overline{w}=\frac{1}{s}\left[\frac{\sinh a(1+y)}{\sinh 2a}-\frac{\sinh\beta(1+y)}{\sinh 2\beta}\right]+\frac{cR}{Rs+D^{-1}}\left(\frac{1}{s}+\frac{1}{(s+\gamma)^2}\right)\left[\frac{\cosh\beta y}{\cosh\beta}-1\right] \tag{28}$$

Taking Inverse Laplace Transform we get w (y, t) as

$$w(y,t)=\frac{cR}{D^{-1}}(1+\gamma)\left[\frac{\cosh ay}{\cosh a}-1\right]+\sum_{n=0}^{\infty}\frac{(-1)^n e^{S_n t}\, n\pi(1+\alpha_0 Rs_n)^2}{2Rs_n(1-\alpha_0 a^2)}\sin\frac{n\pi}{2}(1+y)$$

$$+c\left(\frac{1}{s_n'}+\frac{1}{s_n'+\gamma}\right)\sum_{n=0}^{\infty}\frac{(-1)^n e^{S'_n t}(2n+1)\pi(1+\alpha_0 Rs_n')^2}{(R-\alpha_0 D^{-1}a^2)(Rs_n'+D^{-1})}\cos(2n+1)\frac{\pi}{2}y \tag{29}$$

The Shear stress τ on the upper wall is

$$(\tau)_{y=+1}=\frac{cR}{D^{-1}}(1+\gamma)\left[\frac{a\sinh a}{\cosh a}\right]+\sum_{n=0}^{\infty}\frac{e^{S_n t}\, n\pi(1+\alpha_0 Rs_n)^2}{4Rs_n(1-\alpha_0 a^2)}$$

$$-c\left(\frac{1}{s_n'}+\frac{1}{(s_n'+\gamma)^2}\right)\sum_{n=0}^{\infty}\frac{(-1)^n e^{S'_n t}(2n+1)\pi(1+\alpha_0 Rs_n')^2}{2(R-\alpha_0 D^{-1}a^2)(Rs_n'+D^{-1})}\sin(2n+1)\frac{\pi}{2} \tag{30}$$

The Shear stress Ô on the lower wall is

$$(\tau)_{y=-1}=\frac{cR}{D^{-1}}(1+\gamma)\left[\frac{a\sinh a}{\cosh a}\right]+\sum_{n=0}^{\infty}\frac{e^{S_n t}\, n\pi(1+\alpha_0 Rs_n)^2}{4Rs_n(1-\alpha_0 a^2)}$$

$$+c\left(\frac{1}{s_n'}+\frac{1}{s_n'+\gamma}\right)\sum_{n=0}^{\infty}\frac{(-1)^n\, e^{S_n' t}\,(2n+1)\pi(1+\alpha_0 Rs_n')^2}{2(R-\alpha_0 D^{-1}a^2)\,(Rs_n'+D^{-1})}\sin(2n+1)\frac{\pi}{2} \qquad (31)$$

The flow rate Q is given by

$$Q=\frac{2cR(1+\gamma)}{D^{-1}}\left[\frac{\sinh a}{a\cosh a}-1\right]+\sum_{n=0}^{\infty}\frac{e^{S_n t}\,n\pi(1+\alpha_0 Rs_n)^2}{Rs_n(1-\alpha_0 a^2)}[1-(-1)^n] \qquad (32)$$

$$+c\left(\frac{1}{s_n'}+\frac{1}{(s_n'+\gamma)^2}\right)\sum_{n=0}^{\infty}\frac{(-1)^n\,4e^{S_n' t}\,(1+\alpha_0 Rs_n')^2}{(R-\alpha_0 D^{-1}S_n')\,(Rs_n'+D^{-1})}\sin(2n+1)\frac{\pi}{2}$$

The centerline velocity is given by

$$w(y=0)=\frac{cR(1+\gamma)}{D^{-1}}\left[\frac{1}{\cosh a}-1\right]+\sum_{n=0}^{\infty}\frac{(-1)^n\, e^{S_n t}\,n\pi(1+\alpha_0 Rs_n)^2}{Rs_n(1-\alpha_0 a^2)}\sin\frac{n\pi}{2}$$

$$+c\left(\frac{1}{s_n'}+\frac{1}{s_n'+\gamma}\right)\sum_{n=0}^{\infty}\frac{(-1)^n\, e^{S_n' t}\,(2n+1)\pi(1+\alpha_0 Rs_n')^2}{(R-\alpha_0 D^{-1}S_n')\,(Rs_n'+D^{-1})} \qquad (33)$$

Case: IV

When the pressure gradient is $-\frac{\partial p}{\partial z}=c$

The equation (3.2) takes the form

$$\overline{w}=\frac{1}{s}\left[\frac{\sinh a(1+y)}{\sinh 2a}-\frac{\sinh\beta(1+y)}{\sinh 2\beta}\right]+\frac{cR}{Rs+D^{-1}}\left(\frac{1}{s}\right)\left[\frac{\cosh\beta y}{\cosh\beta}-1\right] \qquad (34)$$

Taking Inverse Laplace Transform wet get w (y, t) is given as

$$w(y,t)=\frac{cR}{D^{-1}}\left[\frac{\cosh ay}{\cosh a}-1\right]+\sum_{n=0}^{\infty}\frac{(-1)^n\, e^{S_n t}\,n\pi(1+\alpha_0 Rs_n)^2}{2Rs_n(1-\alpha_0 a^2)}\sin\frac{n\pi}{2}(1+y)$$

$$+\sum_{n=0}^{\infty}\frac{c(-1)^n\, e^{S_n t}\,(2n+1)\pi(1+\alpha_0 Rs_n')^2}{S_n'(R-\alpha_0 D^{-1}a^2)\,(Rs_n'+D^{-1})}\cos(2n+1)\frac{\pi}{2}y \qquad (35)$$

The Shear stress τ on the upper wall is

$$(\tau)_{y=+1}=\frac{cR}{D^{-1}}\left[\frac{a\sinh a}{\cosh a}\right]+\sum_{n=0}^{\infty}\frac{e^{S_n t}\,n\pi(1+\alpha_0 Rs_n)^2}{4Rs_n(1-\alpha_0 a^2)}$$

$$-\sum_{n=0}^{\infty}\frac{(-1)^n\, e^{S_n t}\,(2n+1)\pi(1+\alpha_0 Rs_n')^2}{2S_n'(R-\alpha_0 D^{-1}a^2)\,(Rs_n'+D^{-1})}\sin(2n+1)\frac{\pi}{2} \qquad (36)$$

The Shear stress τ on the lower wall is

$$(\tau)_{y=-1} = \frac{cR}{D^{-1}}\left[\frac{a\sinh a}{\cosh a}\right] + \sum_{n=0}^{\infty}\frac{e^{S_n t}\, n\pi(1+\alpha_0 Rs_n)^2}{4Rs_n(1-\alpha_0 a^2)}$$

$$+ \sum_{n=0}^{\infty}\frac{c(-1)^n e^{S_n t}(2n+1)\pi(1+\alpha_0 Rs_n')^2}{2S_n'(R-\alpha_0 D^{-1}a^2)(Rs_n'+D^{-1})}\sin(2n+1)\frac{\pi}{2} \qquad (37)$$

The flow rate Q is given by

$$Q = \frac{2cR}{D^{-1}}\left[\frac{\sinh a}{a\cosh a}-1\right] + \sum_{n=0}^{\infty}\frac{e^{S_n t}\, n\pi(1+\alpha_0 Rs_n)^2}{Rs_n(1-\alpha_0 a^2)}[1-(-1)^n]$$

$$+ \sum_{n=0}^{\infty}\frac{c(-1)^n 4e^{S_n' t}(1+\alpha_0 Rs_n')^2}{S_n'(R-\alpha_0 D^{-1}S_n')(Rs_n'+D^{-1})}\sin(2n+1)\frac{\pi}{2} \qquad (38)$$

The centerline velocity at y = 0 is given by

$$w(y=0) = \frac{cR}{D^{-1}}\left[\frac{1}{\cosh a}-1\right] + \sum_{n=0}^{\infty}\frac{(-1)^n e^{S_n t}\, n\pi(1+\alpha_0 Rs_n)^2}{Rs_n(1-\alpha_0 a^2)}\sin\frac{n\pi}{2}$$

$$+ \sum_{n=0}^{\infty}\frac{c(-1)^n e^{S_n' t}(2n+1)\pi(1+\alpha_0 Rs_n')^2}{S_n'(R-\alpha_0 D^{-1}S_n')(Rs_n'+D^{-1})} \qquad (39)$$

DISCUSSION:

In this study we analyse the Start-up flow of a porous medium in a horizontal channel. Initially the flow is assumed to be due to the movement of the boundaries and at time t the boundaries are brought to rest. The subsequent flow is maintained due to a pressure gradient. We studied the problem for three forms of time-dependent pressure gradient and a constant pressure gradient to discuss the flow features. In each case the velocity field, centerline velocity, shear stress on the walls and the flow rate has been calculated for different variations in the governing parameters and their behavior is discussed graphically. The flow phenomena is analyzed for different sets of variations in Viscoelastic parameter α_0, Reynolds number R, Darcy parameter D^{-1} and time t. It is observed that in all cases the velocities are negative except for R variation in the case where the pressure gradient is of the form $c(1 + t\, e^{-\chi})$. In all the four cases, the velocity profiles are bell shaped except for D^{-1} variation, with a maximum attained in the mid plane. It is observed that the magnitude of velocity decreases with increase in Darcy parameter, i.e., lower the permeability of the medium, lesser the velocity in the flow region. Also the magnitude of velocity decreases with increase of time.

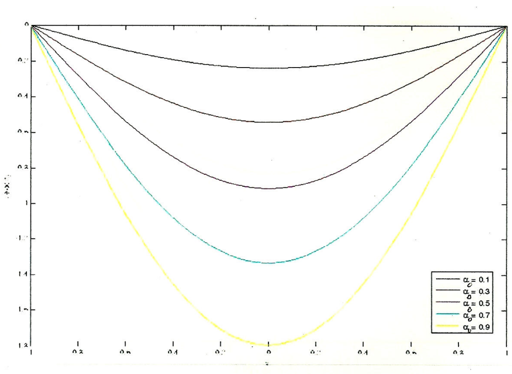

Fig. 1
Variation of Velocity with α_0
t=0.1 R=150, D^{-1} = 3000

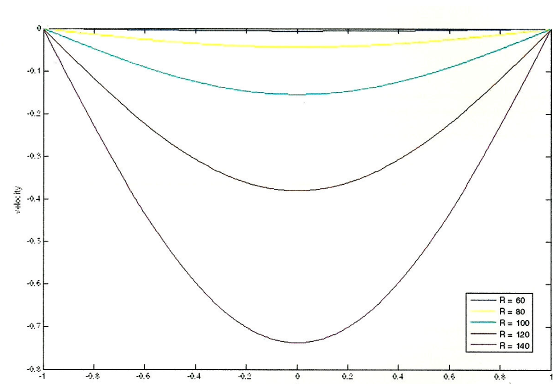

Fig. 2
Variation of Velocity with R
t=1, α_0=1, D^{-1} = 1000

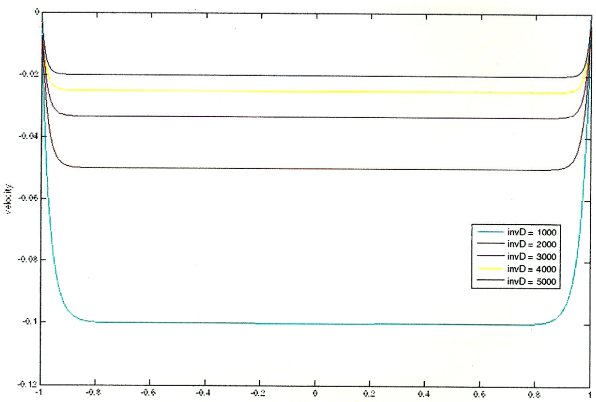

Fig. 3
Variation of Velocity with D^{-1}
$t=1$, $\alpha_0=0.5$, $R=50$

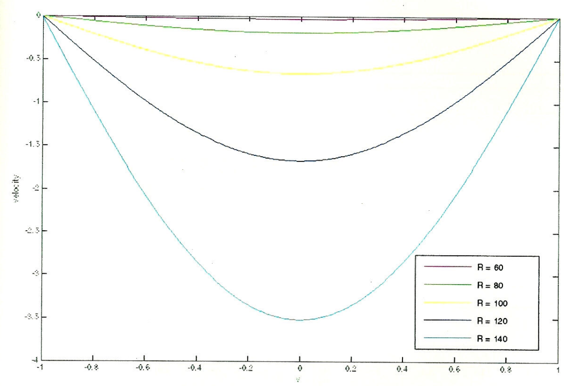

Fig. 6
Variation of Velocity with R
$t=0.5$, $\alpha_0=0.5$, $D^{-1}=1000$

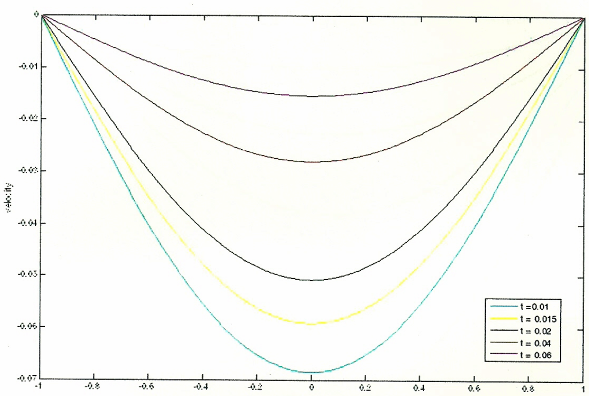

Fig. 4
Variation of Velocity with t
$R=150$, $\alpha_0=0.5$, $D^{-1}=10000$

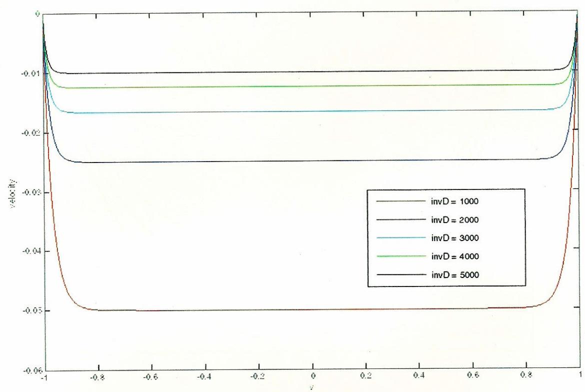

Fig. 7
Variation of Velocity with D^{-1}
$t=1$, $\alpha_0=0.5$, $R=50$

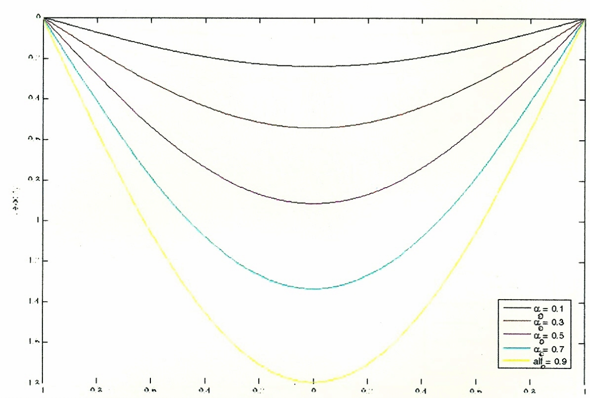

Fig. 5
Variation of Velocity with α_0
$R=150$, $t=0.1$, $D^{-1}=3000$

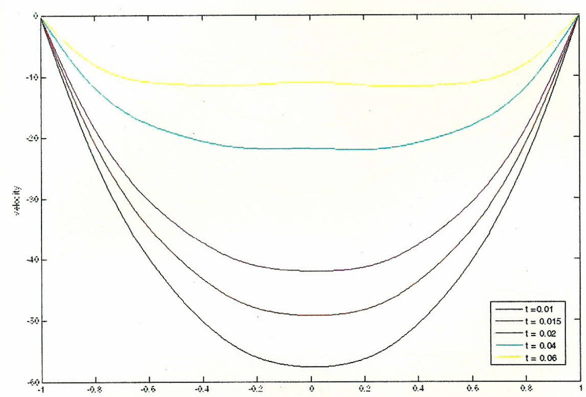

Fig. 8
Variation of Velocity with t
$R=150$, $\alpha_0=0.5$, $D^{-1}=10000$

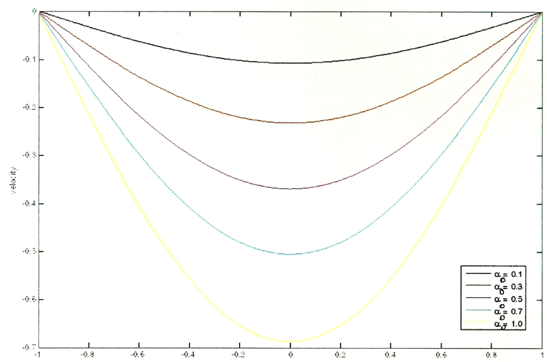

Fig. 9
Variation of Velocity with α_0
t=0.1, R=150, D^{-1} = 3000

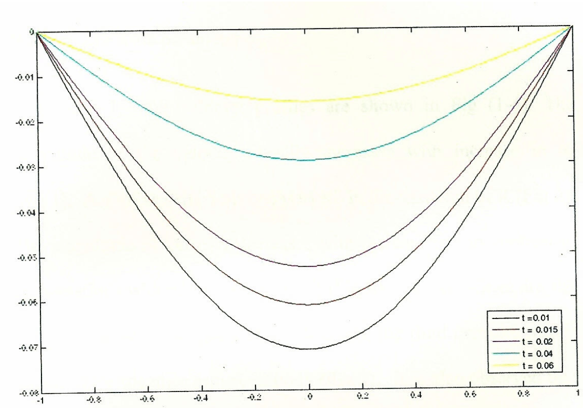

Fig. 12
Variation of Velocity with t
R=150, D^{-1} = 1000, α_0=0.5

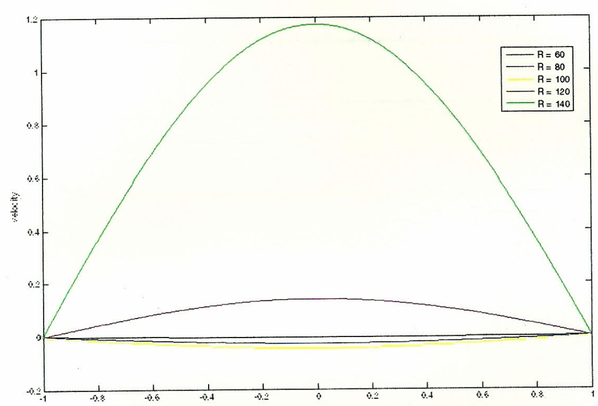

Fig. 10
Variation of Velocity with R
t=1, α_0=1, D^{-1} = 1000

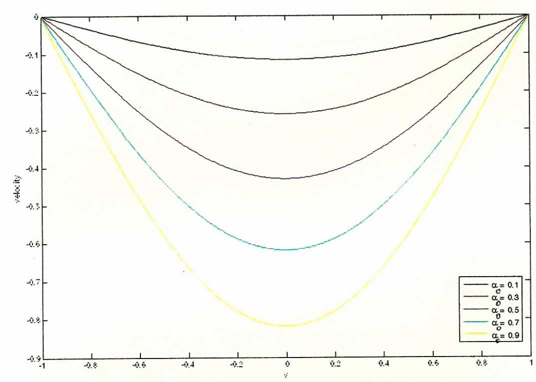

Fig. 13
Variation of Velocity with α_0
t=0.1, R=150, D^{-1}= 3000

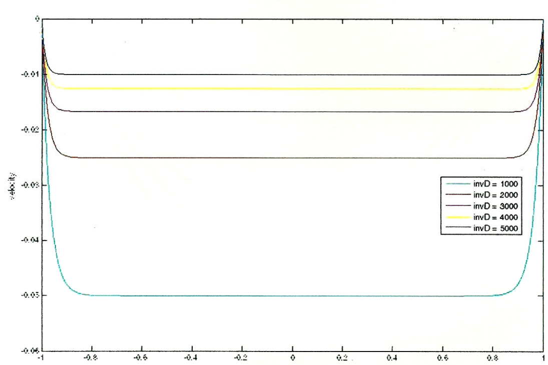

Fig. 11
Variation of Velocity with D^{-1}
t=1, R=50, α_0=0.5

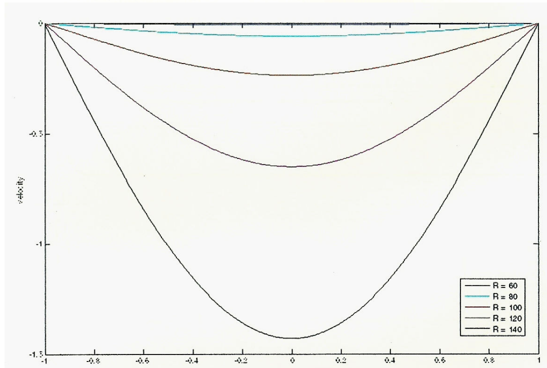

Fig. 14
Variation of Velocity with R
t=1, α_0=1, D^{-1} = 1000

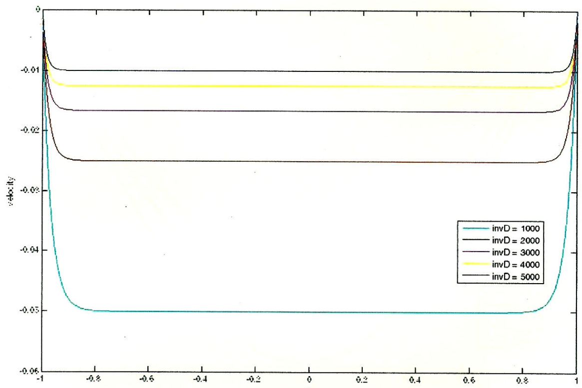

Fig. 15
Variation of Velocity with D^{-1}
t=1, R=50, $\alpha_0 = 0.5$

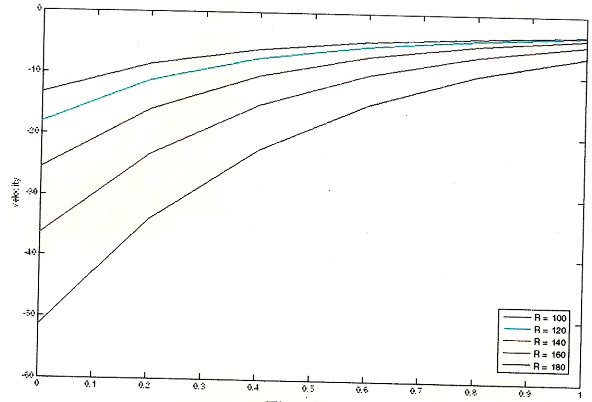

Fig. 18
Variation of Centerline Velocity with R
α_0=0.7, D^{-1} = 1000

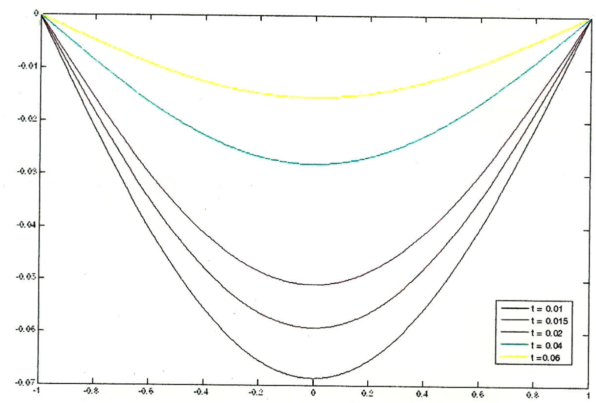

Fig. 16
Variation of Velocity with t
R=150, α_0=0.5, D^{-1} = 10000

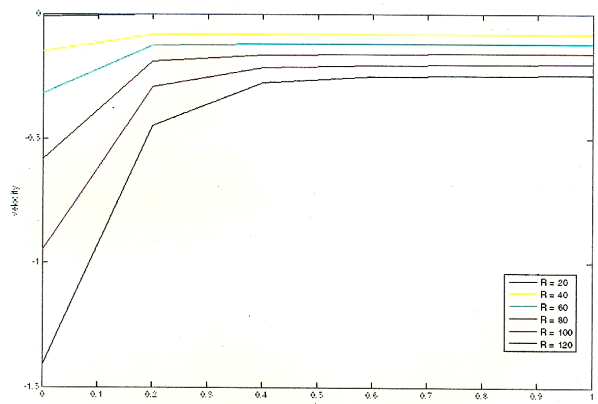

Fig. 19
Variation of centerline velocity with R
α_0=0.1, D^{-1} = 1000

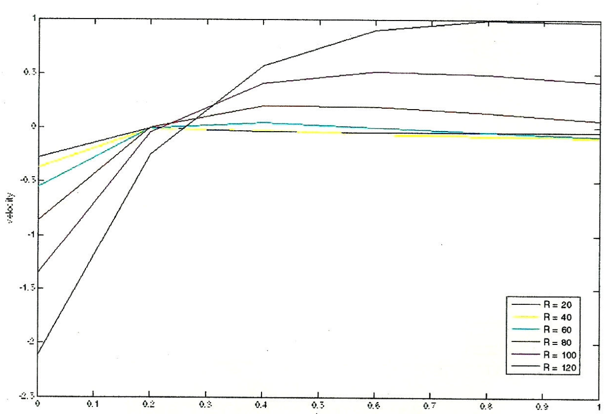

Fig. 17
Variation of centerline velocity with R
α_0=0.5, D^{-1} = 1000

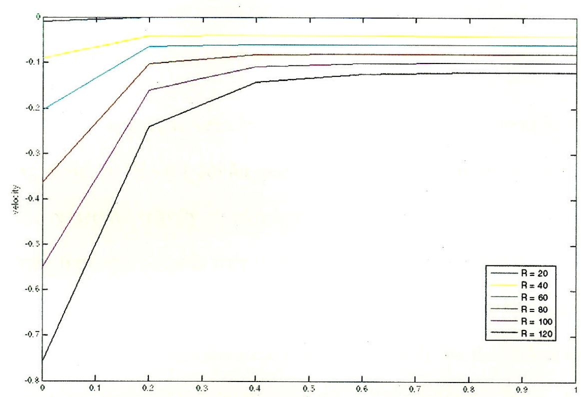

Fig. 20
Variation of centerline velocity with R
α_0=0.05 D^{-1} = 1000

TABLE 1
SHEAR STRESS AT Y=1 IN CASE I

t	a	b	c	d	e	f
0	-88.5477	-192.6308	-329.2515	-106.2995	-247.1237	-435.5470
0.2	-88.244	-188.4552	-321.0352	-106.6524	-241.6898	-424.1426
0.4	-85.0636	-181.3945	-309.8799	-103.0283	-232.5608	-409.0891
0.6	-81.0663	-173.5641	-297.9514	-98.4409	-222.6696	-393.3987
0.8	-76.8374	-165.6147	-285.9770	-93.5663	-212.7047	-377.8046
1.0	-72.6022	-157.7936	-274.2369	-88.6648	-202.9245	-362.5756

	a	b	c	d	e	f
R	80	100	120	80	100	120
D^{-1}	10^3	10^3	10^3	$2x10^3$	$2x10^3$	$2x10^3$

TABLE 2
SHEAR STRESS AT Y=-1 IN CASE I

t	a	b	c	d	e	f
0	-34.4323	-83.7421	-158.0809	-32.8524	-83.8584	-164.1687
0.2	-32.4275	-79.3617	-150.8915	-30.8696	-79.4314	-156.7191
0.4	-30.3076	-74.9860	-143.8234	-28.8001	-75.0182	-149.3862
0.6	-28.2463	-70.7681	-137.0091	-26.8063	-70.7821	-142.3300
0.8	-26.2928	-66.7550	-130.4915	-24.9257	-66.7605	-135.5882
1.0	-24.4620	-62.9589	-124.2806	-23.1675	-62.9604	-129.1661

	a	b	c	d	e	f
R	60	80	100	60	80	100
D^{-1}	10^3	10^3	10^3	$2x10^3$	$2x10^3$	$2x10^3$

TABLE 3
SHEAR STRESS AT Y=1 IN CASE II

t	a	b	c	d	e	f
0	79.3223	90.4617	104.8817	86.4686	97.9375	113.8699
0.2	52.3177	67.5969	84.5323	50.5220	66.3487	85.0332
0.4	41.9912	56.8756	73.5246	41.0061	56.0834	74.0049
0.6	35.8213	50.0436	66.0935	35.2784	49.7144	66.9346
0.8	31.3764	44.9662	60.4129	31.0594	44.9104	61.4987
1.0	27.8849	40.8823	55.7581	27.6914	40.9877	56.9861

TABLE 4
SHEAR STRESS AT Y=-1 IN CASE II

t	a	b	c	d	e	f
0	249.4416	316.2801	373.1324	287.5822	387.5308	482.5627
0.2	88.7686	135.7819	183.5010	82.6538	134.4838	190.6397
0.4	59.3302	92.5390	127.6757	60.5819	101.0303	144.5167
0.6	46.7096	74.2969	103.5444	49.6392	85.0956	123.4764
0.8	38.8343	63.2667	89.3183	42.2700	74.4170	109.5919
1.0	33.1216	55.3455	79.2703	36.6931	66.2890	99.0541

	a	b	c	d	e	f
R	60	80	100	60	80	100
D^{-1}	10^3	10^3	10^3	$2x10^3$	$2x10^3$	$2x10^3$

TABLE 5
SHEAR STRESS AT Y=1 IN CASE III

t	a	b	c	d	e	f
0	31.5431	44.3146	60.1453	49.5172	67.3938	89.2372
0.2	38.7071	55.9877	75.0870	51.1609	74.7115	101.7835
0.4	37.1808	55.6799	76.0712	47.0232	71.1429	98.8901
0.6	34.7032	53.2398	73.7743	43.0193	66.8373	94.3144
0.8	32.1867	50.3783	70.6475	39.3840	62.6085	85.5208
1.0	29.8139	47.5089	67.3468	36.1158	58.6207	84.8460

TABLE 6
SHEAR STRESS AT Y=-1 IN CASE III

t	a	b	c	d	e	f
0	7.5591	19.9184	34.4590	7.4206	20.2274	35.6752
0.2	9.1650	20.7177	34.4164	9.1192	21.2956	36.1231
0.4	9.1320	20.1701	33.3662	8.9656	20.6287	34.9613
0.6	8.6785	19.2249	31.9545	8.4784	19.6165	33.4474
0.8	8.0938	18.1594	30.4348	7.8985	18.5200	31.8542
1.0	7.4761	17.0751	28.9075	7.3024	17.4233	30.2718

	a	b	c	d	e	f
R	60	80	100	60	80	100
D^{-1}	10^3	10^3	10^3	$2x10^3$	$2x10^3$	$2x10^3$

TABLE 7
SHEAR STRESS AT Y=1 IN CASE IV

t	a	b	c	d	e	f
0	79.8583	110.4068	142.2550	95.3446	133.6207	175.1625
0.2	67.0676	95.6753	125.4413	79.4607	116.0292	155.4708
0.4	58.5861	85.5572	113.7106	69.4591	104.1779	141.7658
0.6	52.003	77.5644	104.3992	61.6825	94.6915	130.6399
0.8	46.5843	70.8822	96.5653	55.2648	86.6816	121.1355
1.0	41.9978	65.1302	89.7699	49.8119	79.7351	112.8034

TABLE 8
SHEAR STRESS AT Y=-1 IN CASE IV

t	a	b	c	d	e	f
0	51.3633	89.6460	130.3705	48.6435	78.1213	108.7379
0.2	44.2899	79.2440	116.8029	41.0954	67.5888	95.4369
0.4	39.0830	71.5544	106.8297	35.8459	60.2557	86.1651
0.6	34.8024	65.1591	98.5183	31.6507	54.3832	78.7700
0.8	31.1629	59.6448	91.3128	28.1415	49.4268	72.5191
1.0	28.0112	54.7973	84.9353	25.1365	45.1320	67.0768

	a	b	c	d	e	f
R	60	80	100	60	80	100
D^{-1}	10^3	10^3	10^3	$2x10^3$	$2x10^3$	$2x10^3$

TABLE 9
FLOW RATE IN CASE I

t	a	b	c	d	e	f
0	-35.4315	-19.9677	-7.2443	-85.7815	-65.9482	-47.0645
0.2	-23.4321	-21.4771	-18.4025	-44.2491	-43.9908	-41.1526
0.4	-15.1020	-17.0149	-17.6989	-26.8696	-30.8220	-32.2887
0.6	-9.9604	-12.9478	-15.0085	-17.1948	-22.2306	-25.2778
0.8	-6.6982	-9.8034	-12.3036	-11.3018	-16.2872	-19.8478
1.0	-4.5777	-7.4401	-9.9758	-7.5577	-12.0559	-15.6346

TABLE 10
FLOW RATE IN CASE II

t	a	b	c	d	e	f
0	70.2722	77.3776	79.1293	93.4366	116.7248	135.0013
0.2	2.8881	7.0289	11.5546	0.1999	1.1335	3.2031
0.4	-0.0377	0.4718	1.5116	-0.0893	-0.0816	-0.0063
0.6	-0.2035	-0.1956	-0.0429	-0.1084	-0.1345	-0.1521
0.8	-0.2230	-0.2810	0.3059	-0.1136	-0.1469	-0.1769
1.0	-0.2283	-0.2983	-0.3596	-0.1155	-0.1516	-01858

	a	b	c	d	e	f
R	60	80	100	60	80	100
D^{-1}	10^3	10^3	10^3	$2x10^3$	$2x10^3$	$2x10^3$

TABLE 11
FLOW RATE IN CASE III

t	a	b	c	d	e	f
0	-6.0059	-9.5166	-13.2435	-3.4993	-5.8049	-5672
0.2	-0.7124	-1.5663	-2.8662	-0.2144	-0.3775	-0.6672
0.4	-0.3286	-0.5546	-0.9433	-0.1502	-0.2118	-0.2854
0.6	-0.2710	-0.3847	-0.5408	-0.1336	-0.1801	-0.2267
0.8	-0.2521	-0.3400	-0.4363	-0.1264	-0.1674	-0.2059
1.0	-0.2433	-0.3225	-0.4009	-0.1226	-0.1611	-0.1963

TABLE 12
FLOW RATE IN CASE IV

t	a	b	c	d	e	f
0	-4.3192	43.3568	92.4933	-51.1972	10.0328	76.8931
0.2	-4.0793	22.1472	54.3098	-22.3471	9.2154	50.4611
0.4	-2.4794	14.1962	37.0751	-12.4855	7.5476	37.2550
0.6	-1.5465	9.7867	26.9391	-7.5833	5.8300	28.1939
0.8	-1.0090	6.9419	20.1491	-4.8051	4.4225	21.6098
1.0	-0.6867	4.9940	15.3123	-3.1274	3.3315	16.7042

	a	b	c	d	e	f
R	60	80	100	60	80	100
D^{-1}	10^3	10^3	10^3	$2x10^3$	$2x10^3$	$2x10^3$

We observe that the magnitudes of velocities increase with increase of Reynolds number, R and Viscoelastic parameter α_0.

In case I, the velocity profiles are shown in Fig (1-4). The magnitude of the velocity steadily increases with increase in α_0 (Fig 1). A similar behaviour is observed in the variation of R (Fig 2). The magnitude of velocity decreases with increase in t in contrast to the variations with respect to α_0 and R (Fig 4). The velocities are flat and the flatness of the profiles indicates that the fluid particles in this region move together as a rigid body (Fig 3). It is also observed that the magnitude of velocity decreases with D^{-1}.

In case II, the velocity profiles for variations in α_0, R, D^{-1} are shown in Figs(5-8). They behave in a similar manner as in case I where the pressure gradient is of the form $c(1 + \gamma t)$.

In case III, the velocity profiles for variations in α_0, R, D^{-1}, t are shown Figs (9-12). In this case the velocities are negative for variations of α_0, D^{-1}, t. Fro a variation in R the velocity shows a different behaviour. The velocity is negative for R 100 and suddenly becomes positive for R> 100 (Fig 10), which is in contrast to the behaviour observed in cases II and III.

In case IV, i.e., in the case of constant pressure gradient, the velocity profiles for variations in α_0, R, D^{-1}, t is shown in Figs (13-16). These profiles show a similar behaviour as in case I and II. The centerline velocity profiles with respect to variation in R are drawn in Figs (17-20) for cases I, II, III, IV respectively. In case I the centerline velocity steadily increases for small Reynolds number with time and a steady state is reached at t = 0.4. For large Reynolds numbers there is a sharp increase in the centerline velocity and more time is taken to attain the steady state. In case II the time taken to reach the steady state with R is not following a uniform pattern. In case III, for all values of R the steady state is attained at the same time when R varies from 40 to 100 and more time is taken when R = 120. A similar observation is made in case IV also.

Shear stress τ on the walls have been calculated by setting $\alpha_0 = 0.5$ and tabulated in Tables 1-8. It is observed that for a given Reynolds number R, the magnitude of shear stress decreases with increase in time in all the four cases at both the walls. The shear stresses are negative in case I at both the walls and positive in all the cases II, III and IV.

The flow rate is calculated by setting $\alpha_0 = 0.01$ and tabulated in tables 9-12. It is observed that the flow rate enhances with time in case I, III and IV where it reduces with time in case II. The flow rate increases with increase of Reynolds number in cases I, II and IV. Increase of Reynolds number decreases flow rate in case III. Flow rate decreases with Darcy parameter in cases I and IV and increases in cases II and III.

REFERENCES:

[1] Anderson H.I. and Holmedal L.E, (1995) “Start-up flow in a porous medium channel”, Acta Mecahnica 113, pp. 155-168.

[2] Beavers, G.S. and Joseph, D.D., (1967), J. Flu. Mech. 30, pp. 197.

[3] Brinkman, H.C., (1947), Appl. Sci. Res., A 1, 27.

[4] Darcy H., (1856), “Les fontains publiques delta ville de Dinjoin”, Dalmont, Pariss.

[5] Kazakia J.Y. and Rivlin R.S (1981), Run-up and Spin-up flows in a viscoelastic fluid-I - Rheologia - Acta, 20.

[6] Mahaboob Basha M, (1994), “Viscoelastic fluid flow and the Heat Transfer through a porous medium”, Ph.D., thesis, S.K. University, Anantapur, pp.1-19 and pp. 37-64.

[7] Pattabhi Ramacharyulu N.Ch. and Applala Raju K., (1984), “Run-up flow in a generalized porous medium”, Indian J. Pure and Applied Math., 15(6); pp.665-670.

[8] Ramakrishna D., (1986), “Some problems in the dynamics of fluids with particle suspensions”, Ph.D., Thesis, Osmania University, Hyderabad, P.55.

[9] Rivlin, (1982), Run-up and Spin-up in a Viscoelastic fluids III, Rheologica Acta, 21, pp.213-222.

[10] Sheelam Raji Reddy, (1992), Computational techniques in Transient Magneto-hydrodynamics, Dusty viscous and Run-up flows, Ph.D., thesis, Osmania University, Hyderabad, pp.47-65.

****

